



# The swimming orientation of multicellular magnetotactic prokaryotes and uncultured magnetotactic cocci in magnetic fields similar to the geomagnetic field reveals differences in magnetotaxis between them

Roger Duarte de Melo · Pedro Leão · Fernanda Abreu · Daniel Acosta-Avalos 

Received: 15 May 2019 / Accepted: 10 September 2019 / Published online: 18 September 2019  
© Springer Nature Switzerland AG 2019

**Abstract** Magnetotactic bacteria have intracellular chains of magnetic nanoparticles, conferring to their cellular body a magnetic moment that permits the alignment of their swimming trajectories to the geomagnetic field lines. That property is known as magnetotaxis and makes them suitable for the study of bacterial motion. The present paper studies the swimming trajectories of uncultured magnetotactic cocci and of the multicellular magnetotactic prokaryote ‘*Candidatus Magnetoglobus multicellularis*’ exposed to magnetic fields lower than 80  $\mu\text{T}$ . It was assumed that the trajectories are cylindrical helices and the axial velocity, the helix radius, the frequency and the orientation of the trajectories relative to the applied magnetic field were determined from the experimental trajectories. The results show the paramagnetic model applies well to magnetotactic cocci but not to ‘*Ca. M.*

*multicellularis*’ in the low magnetic field regime analyzed. Magnetotactic cocci orient their trajectories as predicted by classical magnetotaxis but in general ‘*Ca. M. multicellularis*’ does not swim following the magnetic field direction, meaning that for it the inversion in the magnetic field direction represents a stimulus but the selection of the swimming direction depends on other cues or even on other mechanisms for magnetic field detection.

**Keywords** Magnetotaxis · Magnetotactic bacteria · Taxis/tactic responses · Bacterial swimming · Cylindrical helix swimming trajectory

## Introduction

Magnetotactic bacteria (MTB) are microorganisms that biomineralize magnetic nanoparticles of magnetite or greigite surrounded by a membrane and organized in linear chains, conferring a magnetic moment to the bacterial cell body. Because of that magnetic moment MTB show a behavior known as magnetotaxis, that is the alignment of the bacterial body to the magnetic field lines through the passive magnetic torque between its internal magnetic moment and the magnetic field (Kalmijn 1981). MTB include cocci, vibrios, rods, spirilla and multicellular magnetotactic prokaryotes (known as MMPs)

---

**Electronic supplementary material** The online version of this article (<https://doi.org/10.1007/s10482-019-01330-3>) contains supplementary material, which is available to authorized users.

---

R. D. de Melo · D. Acosta-Avalos (✉)  
Centro Brasileiro de Pesquisas Físicas - CBPF, Rua  
Xavier Sigaud 150, Urca, Rio de Janeiro, RJ 22290-180,  
Brazil  
e-mail: dacosta@cbpf.br

P. Leão · F. Abreu  
Instituto de Microbiologia Paulo de Góes, Universidade  
Federal do Rio de Janeiro – UFRJ, Rio de Janeiro,  
RJ 21941-902, Brazil

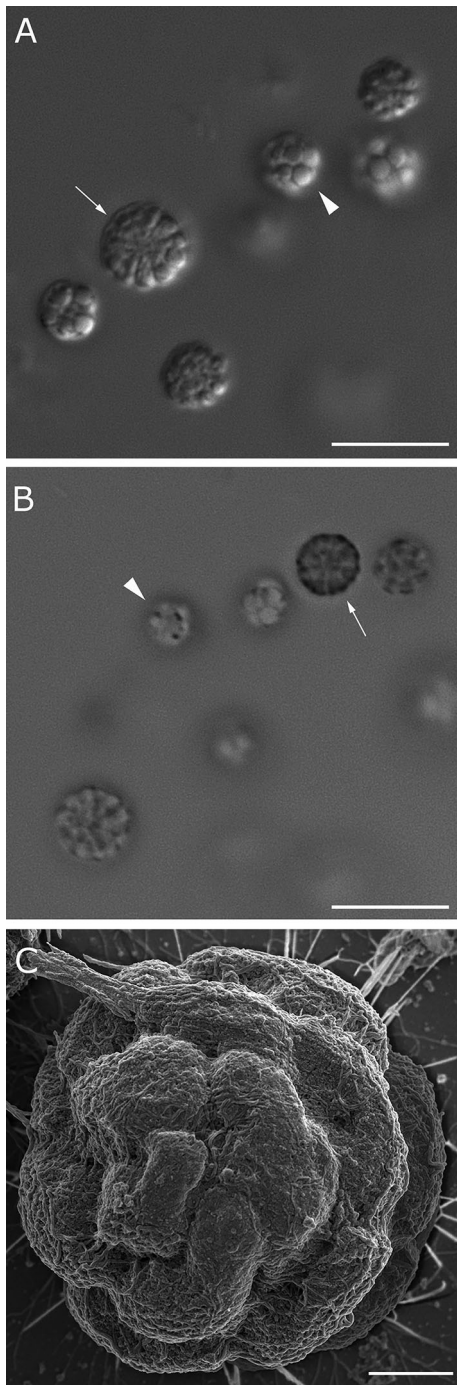


**Fig. 1** Light and electron microscopy images of magnetotactic multicellular prokaryotes. **a** Differential interference contrast microscopy of uncultured magnetotactic prokaryotes showing cell organization in the multicellular microorganisms. **b** Bright-field microscopy image of uncultured magnetotactic prokaryotes showing the presence of magnetosome chains at the periphery of the spherical microorganism. **c** Scanning electron microscopy image showing the helical distribution of the cells that compose the magnetotactic multicellular prokaryote. Note that arrows and arrowheads in (a, b) show microorganisms focused at the center and the top, respectively. Scale bars represent 10  $\mu\text{m}$  in (a, b) and 1  $\mu\text{m}$  in (c)

makes its study by videomicroscopy easier (Fig. 1a, b). The MTB that comprise ‘*Ca. M. multicellularis*’ are Gram-negative cells arranged radially around an acellular compartment (Fig. 1a) and distributed approximately in a spherical helix, wherein the helix axis is also the motion axis (Fig. 1c). Magnetosomes are in planar groups in the cytoplasm close and parallel to the MMP surface (Silva et al. 2007). The magnetosome chains and their associated magnetic moments are almost perpendicular to the spherical helix line, almost following spherical meridians. The resultant magnetic moment in the spherical MMP is directed along the helix axis (Acosta-Avalos et al. 2012). The MMP surface is covered by flagella, which are helical tubes never as long as a helix turn. Its flagellar filaments have average length of  $2.4 \pm 0.5 \mu\text{m}$  and average width of  $15.9 \pm 1.4 \text{ nm}$  (Silva et al. 2007). When several ‘*Ca. M. multicellularis*’ are concentrated in a water drop border, they show clearly two behaviors: they spin continuously and they show the escape motility. The escape motility, also known as “ping-pong” motion, corresponds with a rapid excursion against the magnetic field direction, which decelerates until the microorganism stops and then makes a slower return to the drop border. Greenberg et al. (2005) carried out a detailed study of the escape motility in MMPs. They observed that the escape motility emerges with applied magnetic fields higher than the geomagnetic field, and that the deceleration in the rapid excursion and the acceleration in the return are uniform. Another feature of the escape motility is that the termination distance, i.e. the distance between the beginning of the motion and the point where the MMP stops, depends strongly on the magnetic field. As the escape motility behavior cannot be explained by the conventional passive magnetic torque model,

(Yan et al. 2012). The best studied MMP is ‘*Candidatus Magnetoglobus multicellularis*’ which is a spherical MMP, containing an average number of 17 cells, arranged side by side around a central compartment (Abreu et al. 2007). ‘*Ca. M. multicellularis*’ has a larger diameter than a single cellular MTB and that

Greenberg et al. (2005) proposed a magnetoreceptive internal cellular regulator in MMPs, whose switching is determined by magnetic fields. One can conclude that MMPs have different magnetic behaviors than MTBs and this warrants comparative studies between them.

MTB are easily identified because of their response to the inversion of the local magnetic field direction: after the inversion MTB start to swim following the new magnetic field direction. That is interesting because MTB can be used as a model to study the swimming of microorganisms in response to magnetic fields. Bacteria swim in the Low Reynolds Number regime, where viscous forces and torques act to null the resultant force and torque (Nogueira and Lins de Barros 1995). In that regime several microorganisms swim following a helical trajectory (Crenshaw 1996) whose parametrization in cartesian coordinates ( $x$ ,  $y$ ,  $z$ ) as a function of time, considering the helix axis as the  $x$  axis, can be written as:

$$x(t) = Vt \tag{1a}$$

$$y(t) = R \cos(\omega t) \tag{1b}$$

$$z(t) = R \sin(\omega t) \tag{1c}$$

where  $R$  is the helix radius,  $V$  is the axial velocity and  $\omega = 2\pi f$  is the angular velocity being  $f$  the helix frequency. The movement of ‘*Ca. M. multicellularis*’ has been studied by Almeida et al. (2013) under two different applied magnetic fields (390  $\mu\text{T}$  and 2000  $\mu\text{T}$ ), analyzing the trajectory through Eq. (1). This study showed that for 390  $\mu\text{T}$  the helical parameters were:  $R = 4.5 \pm 1.9 \mu\text{m}$ ,  $V = 87 \pm 22 \mu\text{m/s}$  and  $\omega = 6.3 \pm 1.7 \text{ rad/s}$ , and for 2000  $\mu\text{T}$  are:  $R = 3.8 \pm 1.5 \mu\text{m}$ ,  $V = 110 \pm 26 \mu\text{m/s}$  and  $\omega = 8.0 \pm 2.1 \text{ rad/s}$ . It is interesting to observe that all the parameters showed high standard deviations, typically found in movement studies of ‘*Ca. M. multicellularis*’ environmental samples. That is because each sample analyzed is under different environmental conditions, in contrast to studies based on pure cultures of laboratory strains, which can be grown in reproducible manner and controlled environments. In another study with the same species of MMP (Keim et al. 2018), with magnetic fields from 90 to 3200  $\mu\text{T}$ , it was shown that for magnetic fields lower than 390  $\mu\text{T}$  the parameters are quite different. For example for 150  $\mu\text{T}$  the parameters are:  $R = 8.7 \pm 6.7 \mu\text{m}$ ,

$V = 93 \pm 28 \mu\text{m/s}$  and  $\omega = 7.9 \pm 3.7 \text{ rad/s}$  (Keim et al. 2018). This same study showed that ‘*Ca. M. multicellularis*’ trajectories have high angular standard deviation around the magnetic field direction for magnetic fields lower than 500  $\mu\text{T}$ , contrary to the expected by the magnetotaxis model (Kalmijn 1981; Mao et al. 2014). For other MTB it has been observed that the 2D trajectory was similar to the projection of a 3D helix in the microscope focal plane (see for example Nogueira and Lins de Barros 1995; Lefevre et al. 2009; Zhang et al. 2012; Chen et al. 2015). As far as we know, there are no detailed studies of single cell MTB trajectories in the literature (Zhang et al. 2014; Araujo et al. 2016), there are only the mentioned studies for ‘*Ca. M. multicellularis*’ (Almeida et al. 2013; Keim et al. 2018). In addition, the studies on the trajectory analysis were performed in magnetic fields higher than 90  $\mu\text{T}$ , i.e. values not related to the magnetic field values that magnetotactic microorganisms face in their natural environments.

The goal of the present paper was to study the helical trajectory of ‘*Ca. M. multicellularis*’ and, for the first time, of uncultured magnetotactic cocci when exposed to magnetic fields lower than 80  $\mu\text{T}$  and compare the corresponding results with our current understanding of magnetotaxis.

## Materials and methods

Water and sediment containing ‘*Ca. M. multicellularis*’ were collected from Araruama lagoon, Rio de Janeiro State, Brazil (22°55’24”S, 42°18’12”W) and maintained in glass aquariums in the lab for several weeks. Uncultured magnetotactic cocci were collected from Rodrigo de Freitas lagoon (22°58’S, 43°12’W), an urban lagoon located in Rio de Janeiro city. The sediments were collected in 2007 and have been maintained in a glass aquarium since then, replenishing the aquarium water level from time to time using tap water. The local geomagnetic parameters where ‘*Ca. M. multicellularis*’ and uncultured MTB were maintained are: horizontal component = 18  $\mu\text{T}$ , vertical component = -15  $\mu\text{T}$ , total intensity = 23  $\mu\text{T}$ .

To isolate the magnetic microorganisms for the experiments, a sub-sample was transferred to a specially designed flask containing a lateral capillary aperture and a small magnet to generate a magnetic

field aligned to the capillary aperture (Lins et al. 2003). The studied ‘*Ca. M. multicellularis*’ and uncultured MTB cocci are South-seeking and swam towards the capillary facing the North pole of a magnet. After 5 min, samples were collected with a micropipette.

For light microscopy, ‘*Ca. M. multicellularis*’ samples were obtained by magnetic enrichment (Leão et al. 2018) and observed in a Zeiss Axioplan microscope (Zeiss, Germany) equipped for differential interference contrast and with a digital camera Color View XS. For scanning electron microscopy, samples were prepared according to Leão et al. (2018) and observed on a Zeiss Auriga (Zeiss, Germany) at 1 kV. For transmission electron microscopy observation, uncultured magnetotactic cocci were magnetically concentrated as previously described and transferred to formvar-carbon-coated copper grids. Samples were observed on a Tecnai G20 Microscope (FEI Company) operating at 200 kV.

To record the movements of microorganisms for trajectory analysis, samples were observed with a digital microscope (Celestron model 44340) equipped with a pair of hand-made coils fixed to a microscope glass slide, producing a magnetic field  $\mathbf{B}$  in the focal plane and perpendicular to the optical axis of the microscope (Fig. 2). A  $10\times$  lens was used to observe

‘*Ca. M. multicellularis*’ and an extra digital amplification of 4 times to observe the uncultured magnetotactic cocci. The frame rate to record the movement was 10 fps. A calibration slide for microscopy, consisting of a bar of 1 mm divided in 100 equal parts, was used to convert pixels to micrometers (for ‘*Ca. M. multicellularis*’ 1 pixel =  $1.69\ \mu\text{m}$  and for MTB 1 pixel =  $0.84\ \mu\text{m}$ ). The magnetic field was measured using a 3-axis fluxgate magnetometer (APS model 113). A drop of water was collected from the glass apparatus for magnetic concentration of MTB (Lins et al. 2003) with a micropipette and it was placed on the microscope slide where the magnetic field was already being applied. Video recording started when microorganisms accumulated at the border of the sample drop. When the direction of the magnetic field was inverted, through the inversion of the current in the coils, magnetotactic microorganisms swim following the new magnetic field direction departing from the drop border (see Videos 1 and 2). Several drops of samples were used to obtain a sufficient number of trajectories (usually more than 30). For these experiments, the microscope was oriented in such a way that the geomagnetic field was oriented perpendicular to the coil axis in the focal plane. In other words, assuming that the XY plane corresponds

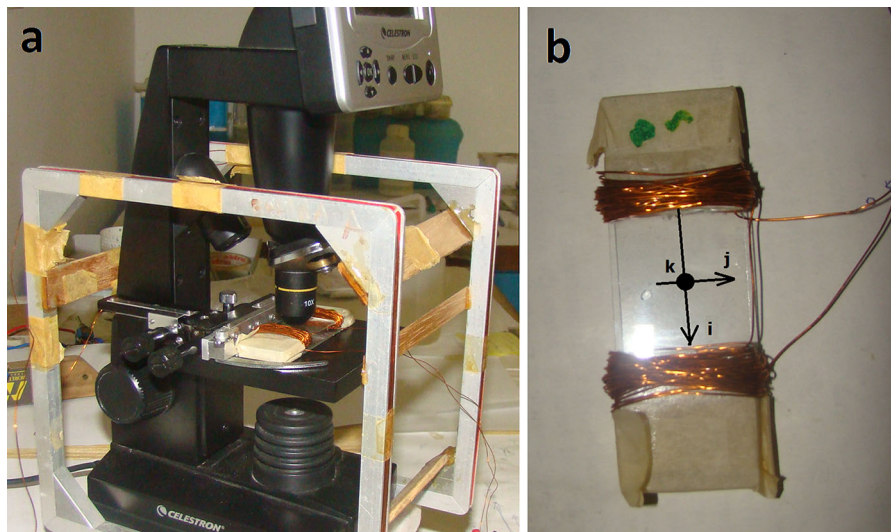


**Fig. 2** **a** Experimental set-up. On the microscope stage is a pair of coils, fixed to a glass microscope slide, used for the generation of the magnetic field. In the figure appears an external set of coils that were not used. **b** Representation of the reference system used in the analysis, drawn on the glass microscope slide.  $\mathbf{i}$ ,  $\mathbf{j}$  and

$\mathbf{k}$  are the Cartesian versors forming an orthonormal basis. The black circle in the middle represents an arrow pointing to the observer and corresponding to the Z axis. The optical plane corresponds to the X–Y plane and Z is directed vertical upside, parallel to the microscope optical axis

to the focal plane and the Z axis is the vertical axis (the microscope optical axis), then:

$$\mathbf{B} = B\mathbf{i} \tag{2a}$$

$$\mathbf{B}_{\text{GEO}} = (18 \mu\text{T}) \mathbf{j} + (15 \mu\text{T}) \mathbf{k} \tag{2b}$$

where  $\mathbf{i}, \mathbf{j}, \mathbf{k}$  are the Cartesian unitary vectors (Fig. 2b),  $\mathbf{B}$  is the magnetic field produced by the coils and  $\mathbf{B}_{\text{GEO}}$  is the geomagnetic field.

Trajectory coordinates were obtained manually, from the recorded videos, for each microorganism frame by frame, using the *ImageJ* software (National Institutes of Health, USA; <https://imagej.nih.gov/ij/>), and later they were analyzed with the *MicroCal Origin* software (OriginLab). It was assumed that the observed trajectories are plane projections of cylindrical helices, being observed only the coordinates X and Y in Eqs. 1. For each trajectory, it was estimated the translational velocity  $V_T$ , the helix frequency  $f$  and the helix radius R. Also for each magnetic field, the distribution of orientation angles  $\theta$  around the magnetic field direction was estimated. To calculate  $\theta$  the following relation was used:  $V_y/V_x = \tan\theta$  (see below). Statistical tests were done with the software *GraphPad InStat* (GraphPad Software Inc.), except the angular statistics, which was done with the software *Oriana* (Kovach Computing Services).

### Interpretation of the 2D projections of the trajectories

The movement of these microorganisms occurs under the Low Reynolds Number regime. For magnetotactic microorganisms, experimental evidence and theoretical models show that they must swim following helical trajectories (see examples of experimental trajectories in Lefevre et al. 2009, Cui et al. 2012; Zhang et al. 2012; Chen et al. 2015; Nogueira and Lins de Barros 1995; and theoretical models in Nogueira and Lins de Barros 1995; Cui et al. 2012; Yang et al. 2012; Kong et al. 2014). Some simulations also showed that the trajectories are composed of two superimposed helices (Klumpp et al. 2019). The simplest helical trajectory is the cylindrical helix, as has been assumed for ‘*Ca. M. multicellularis*’ by Almeida et al. 2013 and Keim et al. 2018, and whose equations are Eqs. (1) where the X axis coincides with the helix axis. The recording of a microorganism swimming in a microscope produce bidimensional

data. Considering that the X axis is parallel to the helix axis and located on the focal plane together with the Y axis, the observed trajectory must be an undulation with parametric Eqs. (1a) and (1c). However, the trajectory is not fully parallel to the magnetic field direction because of thermal perturbations that disorient the bacterial swimming (Kalmijn 1981). In that case the axis of the helical trajectory must be tilted relative to the magnetic field by an angle  $\theta$  and the parametric equations for the X and Y coordinates must be as follows:

$$\begin{aligned} X' &= X \cos \theta + Y \sin \theta \\ &= R \sin \theta \cos(2\pi ft) + V \cdot t \cdot \cos \theta \end{aligned} \tag{3a}$$

$$\begin{aligned} Y' &= -X \sin \theta + Y \cos \theta \\ &= R \cos \theta \cos(2\pi ft) - V \cdot t \cdot \sin \theta \end{aligned} \tag{3b}$$

Equations 3a and 3b represent straight lines with sinusoidal perturbations (Fig. 3). Experimentally, the angle  $\theta$  and the helix parameters V, R and  $f$  can be calculated through Eqs. (3a) and (3b), considering that for the video-microscopy the camera position was adjusted in such a way that the horizontal axis of the frames was aligned to the applied magnetic field  $\mathbf{B}$ . In other words, the  $0^\circ$ – $180^\circ$  line corresponds with the X axis, being the  $0^\circ$  direction directed inside the drop, and the  $90^\circ$ – $270^\circ$  line corresponds with the drop border. In Fig. 3a the drop border is located to the right.

## Results and discussion

Many magnetotactic microorganisms swim in helical trajectories that can be approximated by cylindrical helices. To our knowledge, this trajectory analysis was performed only for ‘*Ca. M. multicellularis*’ at magnetic fields higher than  $90 \mu\text{T}$  (Almeida et al. 2013; Keim et al. 2018). Table 1 shows the results of the trajectories for the uncultured magnetotactic cocci and ‘*Ca. M. multicellularis*’ as a function of the magnetic field. As the experimental setup has two magnetic field components, then the total magnetic field corresponds to the sum of the applied magnetic field  $\mathbf{B}$  and the geomagnetic field (Eqs. 2a and 2b):  $\mathbf{B}_T = B\mathbf{i} + (18 \mu\text{T}) \mathbf{j} + (15 \mu\text{T}) \mathbf{k}$ . Table 1 shows the corresponding intensity of the vector  $\mathbf{B}_T$  for each value of B. For ‘*Ca. M. multicellularis*’ the velocity

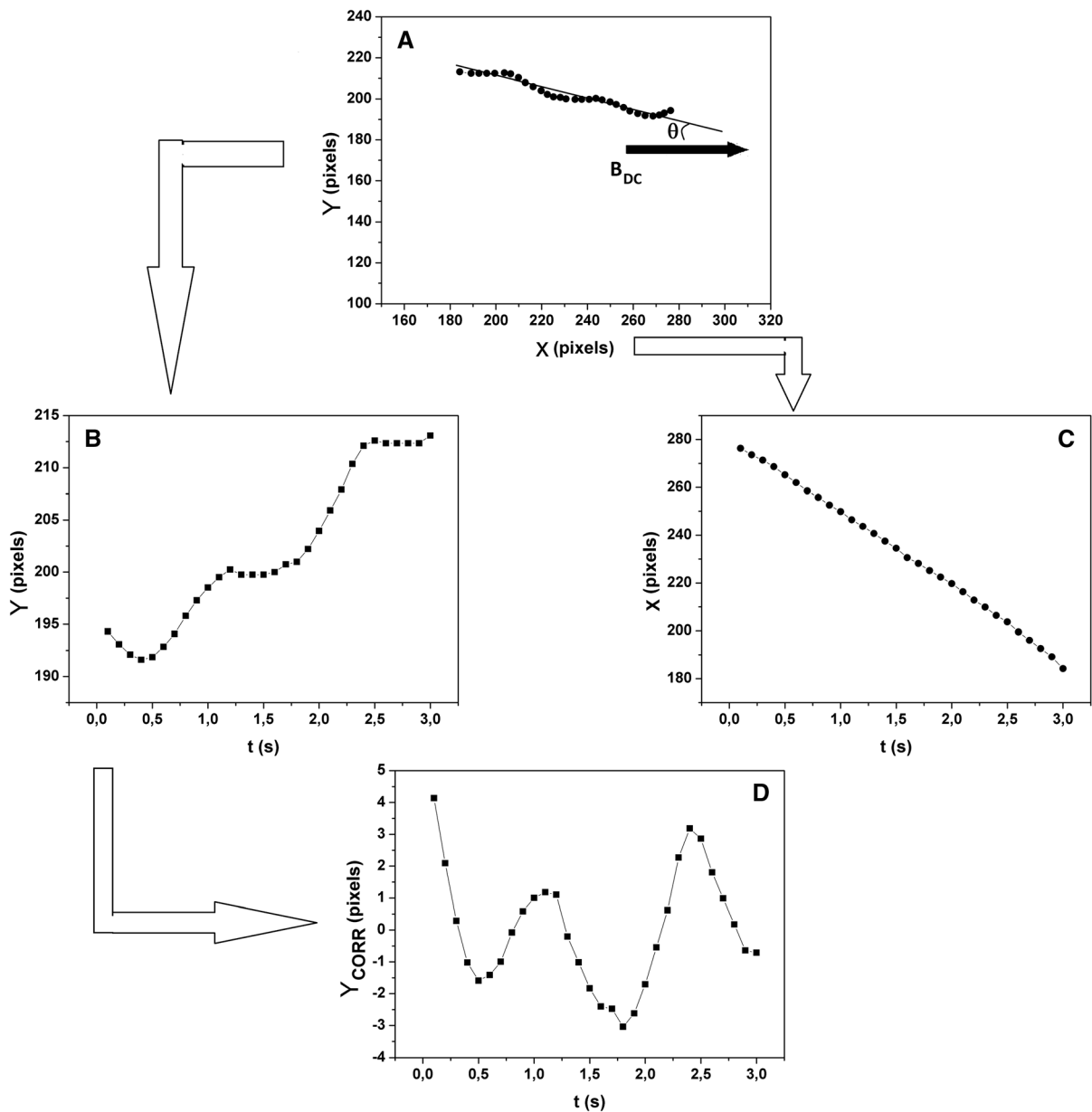


**Fig. 3** Example of a curve analysis for ‘*Ca. Magnetoglobus multicellularis*’. **a** XY plot of the original trajectory. In this figure the drop border is in the right-side, and the ‘*Ca. Magnetoglobus multicellularis*’ moves from right to left. It is represented the direction of  $B$  and the angle  $\theta$  among the trajectory and  $B$ . The trajectory is contrary to the magnetic field because the magnetotactic microorganism is swimming towards the magnetic North pole **b**, **c** Analysis of the individual

coordinates X and Y (respectively) as function of time. A linear fit of these curves was done to calculate the velocities  $V_x$  and  $V_y$ . **d** Resulting curve after the subtraction of the linear tendency ( $V_y t$ ) in the coordinate Y (identified as  $Y_{CORR}$ ). A non-linear fit to Eq. (3b) without the linear tendency was used to calculate the radius R and frequency f. In all figures, the distance is measure in pixels and later was converted to micrometers using a microscope calibration grade

increases for the higher magnetic field, and the frequency and radius do not change among the used magnetic fields. For the uncultured magnetotactic cocci the parameters are statistically similar for the

different magnetic field values. Trajectory frequencies for the uncultured magnetotactic cocci are slightly higher than for ‘*Ca. M. multicellularis*’. The helix

**Table 1** Values of the parameters V, R and f for the helical trajectories obtained from data analysis using Eqs. (3) and the procedure shown in Fig. 3

B (μT)	B <sub>T</sub> (μT)	V ± SD (μm/s)	R ± SD (μm)	f ± SD (Hz)	N
<i>Uncultured magnetotactic cocci</i>					
59	63	89 ± 42 <sup>a</sup>	2.4 ± 1.7 <sup>a</sup>	1.0 ± 0.7 <sup>a</sup>	43
66	69	89 ± 33 <sup>a</sup>	2.7 ± 1.5 <sup>a</sup>	0.8 ± 0.6 <sup>a</sup>	40
72	75	83 ± 20 <sup>a</sup>	2.5 ± 1.6 <sup>a</sup>	1.0 ± 0.6 <sup>a</sup>	48
<i>‘Ca. Magnetoglobus multicellularis’</i>					
59	63	80 ± 18 <sup>A</sup>	6.1 ± 3.2 <sup>A</sup>	0.8 ± 0.3 <sup>A</sup>	37
66	69	81 ± 15 <sup>A</sup>	6.6 ± 3.8 <sup>A</sup>	0.7 ± 0.3 <sup>A</sup>	40
72	75	93 ± 29 <sup>B</sup>	5.6 ± 2.6 <sup>A</sup>	0.9 ± 0.4 <sup>A</sup>	41

B<sub>T</sub> corresponds to the amplitude of the magnetic field vector obtained from the sum of **B** and **B**<sub>GEO</sub>. SD is the standard deviation. N is the number of trajectories analyzed. In the columns, statistical comparison (ANOVA test with multi-comparison test) is shown with superscript letters: equal letters stand for mean values statistically similar (*p* > 0.05) and different letters stand for mean values statistically different (*p* < 0.05)

radius for magnetotactic cocci are lower than those of the trajectories of ‘*Ca. M. multicellularis*’.

Another parameter analyzed was the trajectory orientation relative to the applied magnetic field **B**. Magnetotaxis is recognized because magnetotactic microorganisms react to changes in the magnetic field direction, swimming in trajectories parallel to the magnetic field. As the axial velocity is parallel to the helical trajectory axis, the trajectory angle  $\theta$  relative to the X axis using the velocity components was determined. The angle is relative to the X axis because it corresponds to the direction of the main magnetic field component. The angle  $\theta$  was calculated using Eqs. (3). As the observed movement is projected in the focal plane, the expected angle of orientation  $\theta_{MF}$  is the angle, relative to the X axis, of the magnetic field projected in the focal plane. It was calculated as  $\arctan(18/B)$ , because from Eqs. (2):  $\tan \theta_{MF} = B_{GEO} / Y/B$ . The results are shown in Table 2. It can be seen that the uncultured magnetotactic cocci swim following

approximately the direction of magnetic field projected in the focal plane, as expected for magnetotactic behavior (Frankel and Blakemore 1980), but ‘*Ca. M. multicellularis*’ swims following different directions than that of the magnetic field, with mean angular directions different from  $\theta_{MF}$  and high standard deviations (Fig. 4). Interestingly, some ‘*Ca. M. multicellularis*’ swam close to the line 90°–270° (Fig. 4), that represents the drop border and is far from the angle  $\theta_{MF}$ . Those microorganisms departed from the drop border when the magnetic field **B** direction was inverted, but they do not follow the magnetic field vector B<sub>T</sub>. Table 2 shows that the mean angles for ‘*Ca. M. multicellularis*’ are near to 0° that corresponds with the direction of the applied magnetic field **B**. In some way, ‘*Ca. M. multicellularis*’ reacts to the inversion of magnetic field direction, and swims following only the magnetic field component that change its direction. It appears that ‘*Ca. M. multicellularis*’ uses

**Table 2** Circular statistics for trajectory angles  $\theta$  (the angle among the axial velocity and the magnetic field **B**)

B (μT)	B <sub>T</sub> (μT)	Uncultured magnetotactic cocci $\theta \pm SD$ (°)	‘ <i>Ca. Magnetoglobus multicellularis</i> ’ $\theta \pm SD$ (°)	$\theta_{MF}$ (°)
59	63	24 ± 5.9	7.4 ± 13	19
66	69	22 ± 4.6	3.9 ± 25	17
72	75	19 ± 5.8	5.1 ± 18	16

SD is the Circular Standard Deviation.  $\theta_{MF}$  corresponds to the angle among the DC magnetic field (**B**<sub>GEO</sub> + **B**) and the X axis. For all the groups the Rayleigh test gives *p* < < 0.05, meaning that the angles are not distributed uniformly around the circle but concentrated around the mean angle

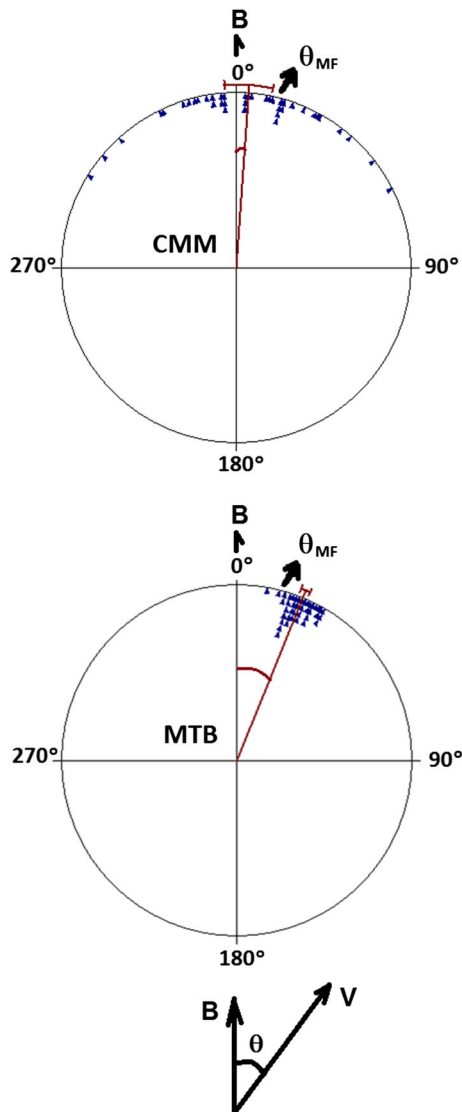


**Fig. 4** Representative circular histograms for ‘*Ca. Magnetoglobus multicellularis*’ and uncultured magnetotactic cocci. They correspond to the applied magnetic field  $B = 66 \mu\text{T}$ . The internal triangles represent the angular data. The applied magnetic field was applied in the  $0^\circ$  direction and is shown with an arrow in the top of that position. The external arrowhead represents  $\theta_{MF}$  that is the angular direction of the total magnetic field. The red line represents the position of the mean trajectory angle between the velocity and the applied magnetic field and the bar on top of it represents the circular standard deviation. In the bottom of the figure is the representation of the angle  $\theta$  between the applied magnetic field  $B$  and the axial velocity  $V$ . Inside the circles: CMM, *Ca. Magnetoglobus multicellularis*; MTB, magnetotactic bacteria

magnetotaxis and another unknown mechanism to detect the geomagnetic field.

As magnetotaxis is related to the presence of the intracellular magnetosome chain(s), because it confers a magnetic moment to the magnetotactic microorganism, it is interesting to discuss their distribution in both uncultured magnetotactic cocci and ‘*Ca. M. multicellularis*’. For the uncultured magnetotactic cocci, transmission electron microscopy images showed that each cell contains two magnetosome chains (Fig. 5). Each magnetosome chain has an average number of 7 nanoparticles (SD = 2, Number of chains = 16). Based on the crystal habit, which is similar to an octahedron in several uncultured magnetotactic cocci (Posfai et al. 2013), and uniform contrast on images, these magnetosomes are probably composed of magnetite. Assuming this mineral composition for the magnetosomes in the uncultured magnetotactic cocci studied here, it is possible to estimate the average magnetic moment in these cells, as done by Frankel and Blakemore (1980). Considering each nanoparticle as a parallelepiped it is possible to calculate its magnetic moment as  $V * M_V$ , where  $V$  is the volume and  $M_V$  is the magnetic moment per unit volume of magnetite ( $0.48 \text{ Am}^2/\text{cm}^3$ ). Each magnetosome has an average length of 115 nm (SD = 22 nm, Number of magnetosomes = 89) and width of 93 nm (SD = 23 nm, Number of magnetosomes = 89), and presents an average magnetic moment of  $5.3 \times 10^{-16} \text{ Am}^2$  (SD =  $2.7 \times 10^{-16} \text{ Am}^2$ , Number of magnetosomes = 89). Each uncultured magnetotactic coccus has an average magnetic moment of  $6.8 \times 10^{-15} \text{ Am}^2$  (SD =  $4.3 \times 10^{-15} \text{ Am}^2$ , Number of cocci = 7) assuming that both magnetosome chains are parallel. If both magnetosome chains are not parallel then the resultant magnetic moment must be lower than  $6.8 \times 10^{-15} \text{ Am}^2$ . Unfortunately, flagella were not observed in the images, probably because it was not preserved during sample preparation. It can be assumed that these magnetotactic cocci have one tuft or two parallel tufts of flagella as has been observed in other magnetotactic cocci (Nogueira and Lins de Barros 1995; Felfoul et al. 2016; Araujo et al. 2016). As both magnetosome chains are not parallel in general, the resultant magnetic moment must present an inclination relative to the tuft or tufts of flagella. The theoretical models to study the magnetotactic movement of cells assume only one magnetosome chain being parallel to (Nogueira and Lins de Barros



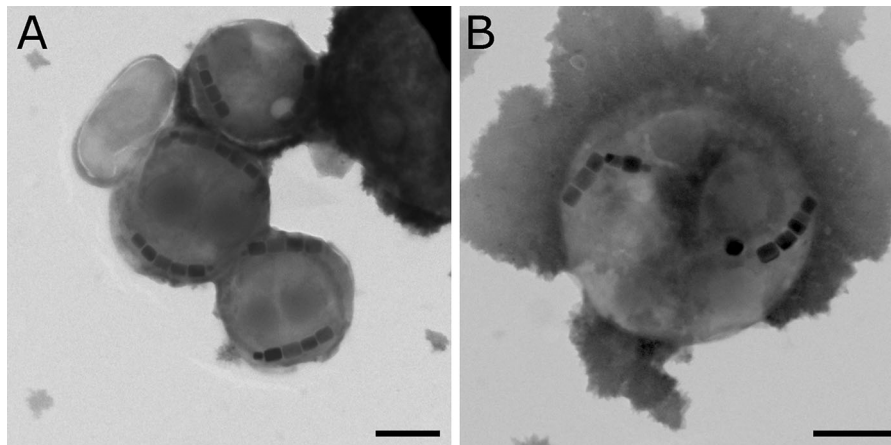


**Fig. 5** Transmission electron microscopy images of uncultured magnetotactic cocci. **a** Uncultured magnetotactic cocci with two parallel magnetosome chains at low magnification. **b** Higher

magnification of an uncultured magnetotactic coccus showing the two perpendicular magnetosome chains in detail. Scale bars indicate 500 nm

1995; Kong et al. 2014) or with a relative inclination to (Yang et al. 2012) the flagella. To consider two magnetosome chains in a MTB motion model an extra magnetic torque must be introduced into the equations analyzed by Nogueira and Lins de Barros (1995) and Yang et al. (2012). It is interesting to observe that any of the mentioned models predicts trajectory frequencies as low as the reported in the present work (Table 1). The distribution of magnetosomes in ‘*Ca. M. multicellularis*’ has been studied using electron microscopy and tridimensional reconstruction of the microorganism (Abreu et al. 2013) and using a theoretical distribution analysis (Acosta-Avalos et al. 2012). It has been shown that ‘*Ca. M. multicellularis*’ presents in each cell several aligned magnetosome chains in the part of the cell close to the external environment (periphery of the spherical multicellular microorganism). As all the constituent cells are organized in a curve similar to a spherical helix, it is possible to analyze the distribution of magnetic moments in that curve and the resultant magnetic moment. Interestingly, Acosta-Avalos et al. (2012) showed that the observed distribution of magnetic moments in ‘*Ca. M. multicellularis*’ corresponds to the minimum magnetic energy distribution, and the total magnetic moment calculated for 15 magnetotactic cells in a *Ca. M. multicellularis* organism was  $22.8 \times 10^{-15} \text{ Am}^2$  (assuming a magnetic moment of  $1.8 \times 10^{-15} \text{ Am}^2$  for each cell). Perantoni et al. (2009) estimate the magnetic moment of ‘*Ca. M. multicellularis*’ using the U-turn technique and found values in

the range from  $5 \times 10^{-15}$  to  $35 \times 10^{-15} \text{ Am}^2$ , showing a distribution with two peaks: one at about  $10 \times 10^{-15} \text{ Am}^2$  and other at about  $20 \times 10^{-15} \text{ Am}^2$ . This multicellular magnetotactic prokaryote shows several short flagella distributed around the whole organism (Silva et al. 2007).

Data shown in Table 2 do not correspond with the orientation angle relative to the magnetic field and are not appropriate for the calculation of the average cosine of the orientation angle as done by Kalmijn (1981) and Mao et al. (2014) to measure the orientation degree. Instead, we calculated the average of  $\cos(\theta - \theta_{MF})$  because the angle  $(\theta - \theta_{MF})$  measures the orientation relative to the resulting magnetic field. The results for  $\langle \cos(\theta - \theta_{MF}) \rangle$  and for the variance  $\sigma^2$  are shown in Table 3. As can be seen, the uncultured magnetotactic cocci show  $\langle \cos(\theta - \theta_{MF}) \rangle$  values of about 0.99 while ‘*Ca. M. multicellularis*’ shows lower values. Mao et al. (2014) reported similar  $\langle \cos\theta \rangle$  values for a magnetotactic ovoid cocci and for ‘*Candidatus Magnetobacterium bavaricum*’ collected from a German lake, for the same range of magnetic fields as shown in Table 3. The magnetic moment measured for ‘*Ca. M. bavaricum*’ was 10 times larger than that obtained for the magnetotactic ovoid cocci and presented similar values of  $\langle \cos\theta \rangle$  when cells were exposed to magnetic fields higher than  $60 \mu\text{T}$  (Mao et al. 2014). Table 3 shows that this is not the case for ‘*Ca. M. multicellularis*’ when compared to the uncultured magnetotactic cocci of our study. Values

**Table 3** Statistics for the orientation relative to  $\mathbf{B}_T$ .  $\langle \cos(\theta - \theta_{MF}) \rangle$  is the average value of  $\cos(\theta - \theta_{MF})$  and  $\sigma^2$  is the variance. Using Eq. (4) is calculated the energy rate  $X = mB/kT$  for every magnetic field  $B_T$

$B_T$ ( $\mu T$ )	Uncultured magnetotactic cocci	' <i>Ca. Magnetoglobus multicellularis</i> '	$X$	
	$\langle \cos(\theta - \theta_{MF}) \rangle \pm \sigma^2$	$\langle \cos(\theta - \theta_{MF}) \rangle \pm \sigma^2$	MTB	CMM
63	$0.993 \pm 0.0003$	$0.944 \pm 0.005$	145	18
69	$0.994 \pm 0.00004$	$0.882 \pm 0.054$	167	9
75	$0.994 \pm 0.0001$	$0.931 \pm 0.014$	167	15

of  $\langle \cos(\theta - \theta_{MF}) \rangle$  for '*Ca. M. multicellularis*' were lower than those for the uncultured magnetotactic cocci. However, it was expected that this multicellular organism showed, at least, similar values of orientation in comparison to those obtained for the uncultured magnetotactic cocci because '*Ca. M. multicellularis*' have magnetic moments about 4 times superior to the magnetic moment calculated for the uncultured magnetotactic cocci reported in this work.

The combination of  $\langle \cos(\theta - \theta_{MF}) \rangle$  and  $\sigma^2$  permits the determination of the energy quotient  $X = mB/kT$  where  $mB$  is the magnetic energy (being  $m$  the magnetic moment and  $B$  the magnetic field) and  $kT$  represents the thermal energy (being  $k$  the Boltzmann constant and  $T$  the absolute temperature). Assuming that the microorganism magnetic moment is parallel to its motility axis Kalmijn (1981) showed that  $\langle \cos(\theta - \theta_{MF}) \rangle = \coth(X) - 1/X$  and  $\sigma^2 = 1 - \coth^2(X) + 1/X^2$ . Simple math permits the formulation that:

$$X = (2 \langle \cos(\theta - \theta_{MF}) \rangle) / (1 - \langle \cos(\theta - \theta_{MF}) \rangle^2 - \sigma^2) \quad (4)$$

The results for  $X$  as function of  $B_T$  are shown in Table 3. The values of  $X$  for '*Ca. M. multicellularis*' are lower than the values for the magnetotactic cocci, meaning that '*Ca. M. multicellularis*' use less magnetic energy in the magnetic orientation of the trajectory compared to the magnetic energy used by the uncultured magnetotactic cocci. However, '*Ca. M. multicellularis*' should present higher values of  $X$  because its magnetic moment is larger than that of magnetotactic cocci. From that values of  $X$  is possible to calculate  $m/kT$  for each magnetic field value, considering that  $kT \approx 4.1 \times 10^{-21}$  J for  $T = 300$  K. The following average values for  $m/kT$  can be obtained:  $\approx 2.4 \times 10^6$  for the uncultured

magnetotactic cocci and  $\approx 0.2 \times 10^6$  for '*Ca. M. multicellularis*', producing values for  $m$  of  $\approx 9 \times 10^{-15}$  Am<sup>2</sup> for the uncultured magnetotactic cocci and  $\approx 8 \times 10^{-16}$  Am<sup>2</sup> for '*Ca. M. multicellularis*'. Those values are underestimated for '*Ca. M. multicellularis*' and for the magnetotactic coccus are similar to the average magnetic moment obtained through the electron microscopy analysis of magnetosomes. This shows that the swimming behavior of '*Ca. M. multicellularis*' under magnetotactic stimulus is notably different from the same behavior of uncultured magnetotactic cocci. In particular, the paramagnetic model developed by Kalmijn (1981) applies well to some unicellular MTB (see Kalmijn 1981 and Mao et al. 2014) but does not applies to '*Ca. M. multicellularis*' producing a less accurate magnetic moment estimative. A similar conclusion was obtained by Keim et al. (2018) analyzing only  $\langle \cos\theta \rangle$  as a function of  $B$ . Kalmijn (1981) showed the application of the method in natural samples of MTB and obtained good values compared with other estimations. However, Kalmijn (1981) mentioned that the paramagnetic method must be applied to the study of the orientation of a single MTB cell and not to the orientation of several bacteria. The use of the paramagnetic model has been criticized as giving a magnetic moment estimative different from the value obtained directly from the magnetosome chain and from other non-statistical methods in the MTB *Magnetospirillum magneticum* strain AMB-1 (Nadkarni et al. 2013). Mao et al. (2014) compared different methods to estimate the magnetic moment in '*Ca. M. bavaricum*' and natural samples of an ovoid coccus, and showed that the paramagnetic model produced similar magnetic moment values to the estimative from the magnetosome chain for '*Ca. M. bavaricum*' but produced different values for the ovoid cocci. In the present work, the paramagnetic model was used in a

different way: the ratio between the magnetic and thermal energy (Eq. 4) was obtained for the first time by combining the equations for  $\langle \cos\theta \rangle$  and  $\sigma^2$ , and from the value of the ratio the magnetic moment was obtained. Our results show a good agreement between the paramagnetic model and the estimative from the magnetosome chain for the noncultured magnetotactic cocci but different values for '*Ca. M. multicellularis*'. It may be that this difference is because of the complex distribution of magnetic moments around the body of '*Ca. M. multicellularis*'.

Magnetotactic microorganisms live under the influence of the geomagnetic field. The mean worldwide value for  $B_{\text{GEO}}$  is about 50  $\mu\text{T}$ , but Rio de Janeiro, Brazil, is located in the South Atlantic Anomaly region, where the geomagnetic field has the lowest value of approximately 22  $\mu\text{T}$  (Pinto Jr et al. 1992). It is interesting to study the behavior of magnetotactic microorganisms under very low magnetic field intensities similar to that of  $B_{\text{GEO}}$ . To our knowledge, this is the first study that characterizes the swimming trajectories of magnetotactic microorganisms exposed to magnetic fields lower than 80  $\mu\text{T}$ . Keim et al. (2018) analyzed the trajectories of '*Ca. M. multicellularis*' under magnetic field of different values, with 90  $\mu\text{T}$  as the lowest value. On the other hand, the behavior of several magnetotactic bacteria has been studied under 50  $\mu\text{T}$  (Bennet et al. 2014 and Lefevre et al. 2014). However, the aim of these studies (Bennet et al. 2014 and Lefevre et al. 2014) was to understand magneto-aerotaxis, and for that, the speed was measured and the trajectory was not analyzed. The trajectory frequencies observed for uncultured magnetotactic cocci are much lower than frequencies associated to flagellar rotation, of approximately 100 Hz (Berg 2003). The trajectory period was approximately 1 s (frequency of about 1 Hz) and 1.2 s (frequency of about 0.8 Hz), for the uncultured magnetotactic cocci and '*Ca. M. multicellularis*', respectively.

The axial velocity measured for both microorganisms are in accordance to the velocity measured in other MTB (Kalmijn 1981; Almeida et al. 2013; Zhang et al. 2014; Keim et al. 2018). '*Ca. M. multicellularis*' showed lower velocities (about 80  $\mu\text{m/s}$ ) than that of the magnetotactic cocci (about 90  $\mu\text{m/s}$ ), which may be related to the flagella type of each microorganism: '*Ca. M. multicellularis*' presents short flagella distributed around their spherical bodies and magnetotactic cocci generally present one or two

tufts of flagella (Silva et al. 2007; Lefevre et al. 2010; Nogueira and Lins de Barros 1995; Felfoul et al. 2016; Araujo et al. 2016). '*Ca. M. multicellularis*' moves as a single microorganism with flagellar movement highly coordinated among all the MTB that compose it (Silva et al. 2007).

The magnetotactic orientation determined by the angle  $\theta$  seems to be effective in MTB as shown in Fig. 4, where it was observed that bacterial trajectories approximately follow the magnetic field direction. On the other hand, '*Ca. M. multicellularis*' does not follow the magnetic field direction, but responds to the inversion of the applied magnetic field  $B$ , presenting a higher dispersion in the chosen direction. It appears that in the presence of low magnetic fields the magnetic torque is more effective in unicellular MTB to determine their swimming direction, and in '*Ca. M. multicellularis*' the magnetic torque is not effective enough to determine the swimming direction. Keim et al. (2018) showed that for magnetic fields higher than 1000  $\mu\text{T}$  those microorganisms effectively orient their trajectories to the magnetic field direction, decreasing strongly the angular dispersion around the magnetic field, in contrast to what was observed in the present research for magnetic fields lower than 80  $\mu\text{T}$ . '*Ca. M. multicellularis*' has a complex distribution of magnetosome chains around the axis of a spherical helix (Acosta-Avalos et al. 2012) producing a resultant magnetic moment directed in that axis. It is notable that '*Ca. M. multicellularis*' has a magnetic moment of about 4 times larger than that of the MTB coccus, meaning that the magnetic torque produced by the resultant magnetic field  $B_T$  must be also higher. It may be that in '*Ca. M. multicellularis*' the magnetic torque is compared with other stimuli while swimming and that the observed swimming direction is the result of the analysis of several ambient cues, as has been proposed in a recent study by Keim et al. (2018). Our results suggest that for '*Ca. M. multicellularis*' the inversion in the magnetic field direction represents a stimulus but the selection of the swimming direction depends on other ambient cues or even on another magnetic field detection mechanism. It seems that '*Ca. M. multicellularis*' does not sense the geomagnetic field in a passive taxis, as in magnetotaxis, determined only by the torque among the magnetic moment of the magnetosome chain and the applied magnetic field (Frankel and Blakemore 1980; Nogueira and Lins de Barros 1995). Magnetotaxis works together with

aerotaxis in a taxis known as magneto-aerotaxis (Lefevre et al. 2014). The observed orientation behavior of ‘*Ca. M. multicellularis*’ must not affect its search for places with optimum oxygen concentration, because at longer distances than those observed in our experiments the microorganisms must be able to orient their swimming trajectories to the geomagnetic field. Even if they do not optimally orient their trajectories to the magnetic field direction, eventually aerotaxis conducts ‘*Ca. M. multicellularis*’ to the oxic-anoxic transition zone. Our results relating to the magnetic orientation of the swimming trajectory show that in ‘*Ca. M. multicellularis*’ the magnetic torque is not as effective as in the uncultured magnetotactic cocci, a counterintuitive result because ‘*Ca. M. multicellularis*’ has a bigger resultant magnetic moment that implies that the resultant magnetic torque in its body is also bigger than that in the magnetotactic cocci. ‘*Ca. M. multicellularis*’ has been considered in discussions about magnetoreception processes in magnetotactic microorganisms, from the analysis of the escape motility behavior (Greenberg et al. 2005) to the finding of a radical pair mechanisms that has been associated with light-dependent magnetoreception (De Melo and Acosta-Avalos 2017). Interestingly the orientation behavior of ‘*Ca. M. multicellularis*’, as observed in the circular histogram (Fig. 4), is similar to the circular histograms observed for animals in magnetoreception experiments (see for example the circular histograms in Wiltshcko and Wiltshcko 2006).

## Conclusion

In conclusion, the present study shows the first measurements of the helical trajectory parameters of unicellular uncultured magnetotactic cocci and ‘*Ca. M. multicellularis*’ under magnetic field intensities lower than 80  $\mu\text{T}$ . The calculation of the magnetic moment using the paramagnetic model developed for MTB produced satisfactory values for the unicellular uncultured magnetotactic cocci. However it was not adequate for the multicellular organism ‘*Ca. M. multicellularis*’, suggesting that that model does not apply to MMPs. Our results show that for low magnetic fields the uncultured magnetotactic cocci orient their trajectories as classical magnetotaxis predicts. On the other hand, in general, in low magnetic fields ‘*Ca. M. multicellularis*’ does not swim

following the magnetic field lines, thus the inversion in the magnetic field direction represents a stimulus but the selection of the swimming direction depends on other cues or even on other mechanisms for magnetic field detection.

**Acknowledgements** D. Acosta-Avalos acknowledges financial support from Fundação do Amparo à Pesquisa do Rio de Janeiro (FAPERJ). R. D. de Melo thanks Conselho Nacional de Desenvolvimento Científico e Tecnológico (CNPq) for PIBIC grant. F. Abreu acknowledges support from FAPERJ, Conselho Nacional de Desenvolvimento Científico e Tecnológico (CNPq), Coordenação de Aperfeiçoamento de Pessoal de Nível Superior (CAPES) and thanks to the microscopy facilities CENABIO-UFRJ and UniMicro-UFRJ.

**Authors contributions** RDM executed experimental work related to the movement recording and obtained the trajectory coordinates, DAA and RDM designed experimental work, PL and FA executed the transmission electron microscopy, DAA and FA conducted data analyses and wrote the manuscript.

**Data availability** The datasets generated during the current study are available from the corresponding author on reasonable request.

## Compliance with ethical standards

**Conflict of interest** The authors declare that they have no conflict of interest.

## References

- Abreu F, Martins JL, Silveira TS, Keim CN, Lins de Barros HGP, Gueiras-Filho F, Lins U (2007) ‘*Candidatus Magnetoglobus multicellularis*’, a multicellular magnetotactic prokaryote from a hypersaline environment. *Int J Syst Evol Microbiol* 57:1318–1322
- Abreu F, Silva KT, Leao P, Guedes IA, Keim CN, Farina M, Lins U (2013) Cell adhesion, multicellular morphology, and magnetosome distribution in the multicellular magnetotactic prokaryote *Candidatus Magnetoglobus multicellularis*. *Microsc Microanal* 19:535–543
- Acosta-Avalos D, Azevedo LMS, Andrade TS, Lins de Barros H (2012) Magnetic configuration model for the multicellular magnetotactic prokaryote *Candidatus Magnetoglobus multicellularis*. *Eur Biophys J* 41:405–413
- Almeida FP, Viana NB, Lins U, Farina M, Keim CN (2013) Swimming behaviour of the multicellular magnetotactic prokaryote ‘*Candidatus Magnetoglobus multicellularis*’ under applied magnetic fields and ultraviolet light. *Antonie Van Leeuwenhoek* 103:845–857
- Araujo ACV, Morillo V, Cypriano J et al (2016) Combined genomic and structural analyses of a cultured magnetotactic bacterium reveals its niche adaptation to a dynamic environment. *BEM Genom* 17(Suppl 8):726

- Bennet M, McCarthy A, Fix D, Edwards MR, Repp F, Vach P, Dunlop JWC, Sitti M, Buller GS, Klumpp S, Faivre D (2014) Influence of magnetic fields on magneto-aerotaxis. *PLoS ONE* 9:e101150
- Berg HC (2003) The rotary motor of bacterial flagella. *Annu Rev Biochem* 72:19–54
- Chen YR, Zhang R, Du HJ, Pan HM, Zhang WY, Zhou K, Li JH, Xiao T, Wu LF (2015) A novel species of ellipsoidal multicellular magnetotactic prokaryotes from Lake Yuehu in China. *Environ Microbiol* 17:637–647
- Crenshaw HC (1996) A new look at locomotion in microorganisms: rotating and translating. *Am Zool* 36:608–618
- Cui Z, Kong D, Pan Y, Zhang K (2012) On the swimming motion of spheroidal magnetotactic bacteria. *Fluid Dyn Res* 44:055508
- De Melo RD, Acosta-Avalos D (2017) Light effects on the multicellular magnetotactic prokaryote ‘*Candidatus Magnetoglobus multicellularis*’ are cancelled by radiofrequency fields: the involvement of radical pair mechanisms. *Antonie Van Leeuwenhoek* 110:177–186
- Felfouf O, Mohammadi M, Taherkhani S et al (2016) Magneto-aerotactic bacteria deliver drug-containing nanoliposomes to tumour hypoxic regions. *Nat Nanotechnol* 11:941–947
- Frankel RB, Blakemore RP (1980) Navigational compass in magnetic bacteria. *J Mag Mag Mater* 15–18:1562–1564
- Greenberg M, Canter K, Mahler I, Tornheim A (2005) Observation of magnetoreceptive behavior in a multicellular magnetotactic prokaryote in higher than geomagnetic fields. *Biophys J* 88:1496–1499
- Kalmijn AJ (1981) Biophysics of geomagnetic field detection. *IEEE Trans Magn MAG-17*: 1113–1124
- Keim CN, Martins JL, Abreu F, Rosado AS, Lins de Barros HGP, Borojevic R, Lins U, Farina M (2004) Multicellular life cycle of magnetotactic prokaryotes. *FEMS Microbiol Lett* 240:203–208
- Keim CN, De Melo RD, Almeida FP, Lins de Barros HGP, Farina M, Acosta-Avalos D (2018) Effect of applied magnetic fields on motility and magnetotaxis in the uncultured magnetotactic multicellular prokaryote ‘*Candidatus Magnetoglobus multicellularis*’. *Environ Microbiol Rep* 10:465–474
- Klumpp S, Lefevre CT, Bennet M, Faivre D (2019) Swimming with magnets: from biological organisms to synthetic devices. *Phys Rep* 789:1–54
- Kong D, Lin W, Pan Y, Zhang K (2014) Swimming motion of rod-shaped magnetotactic bacteria: the effects of shape and growing magnetic moment. *Front Microbiol* 5:8
- Leão P, Gueiros-Filho FJ, Bazylinski DA, Lins U, Abreu F (2018) Association of magnetotactic multicellular prokaryotes with *Pseudoalteromonas* species in a natural lagoon environment. *Antonie Van Leeuwenhoek* 111:2213–2223
- Lefevre CT, Bernadac A, Yu-Zhang K, Pradel N, Wu LF (2009) Isolation and characterization of a magnetotactic bacterial culture from the Mediterranean Sea. *Environ Microbiol* 11:1646–1657
- Lefevre CT, Santini CL, Bernadac A, Zhang WJ, Li Y, Wu LF (2010) Calcium ion-mediated assembly and function of glycosylated flagellar sheath of marine magnetotactic bacterium. *Mol Microbiol* 78:1304–1312
- Lefevre CT, Bennet M, Landau L, Vach P, Pignol D, Bazylinski DA, Frankel RB, Klumpp S, Faivre D (2014) Diversity of Magneto-aerotactic behaviors and oxygen sensing mechanisms in cultured magnetotactic bacteria. *Biophys J* 107:527–538
- Lins U, Freitas F, Keim CN, Lins de Barros H, Esquivel DMS, Farina M (2003) Simple homemade apparatus for harvesting uncultured magnetotactic microorganisms. *Braz J Microbiol* 34:111–116
- Mao X, Egli R, Petersen N, Hanzlik M, Zhao X (2014) Magnetotaxis and acquisition of detrital remanent magnetization by magnetotactic bacteria in natural sediment: first experimental results and theory. *Geochem Geophys Geosyst* 15:255–283
- Nadkarni R, Barkley S, Fradin C (2013) A comparison of methods to measure the magnetic moment of magnetotactic bacteria through analysis of their trajectories in external magnetic fields. *PLoS ONE* 8:e82064
- Nogueira FS, Lins de Barros HGP (1995) Study of the motion of magnetotactic bacteria. *Eur Biophys J* 24:13–21
- Pan Y, Lin W, Li J, Wu W, Tian L, Deng C, Liu Q, Zhu R, Winklhofer M, Petersen N (2009) Reduced efficiency of magnetotaxis in magnetotactic coccoid bacteria in higher than geomagnetic fields. *Biophys J* 97:986–991
- Perantoni M, Esquivel DMS, Wajnberg E, Acosta-Avalos D, Cernicchiaro G, Lins de Barros H (2009) Magnetic properties of the microorganism *Candidatus Magnetoglobus multicellularis*. *Naturwissenschaften* 96:685–690
- Pinto O Jr, Gonzalez WD, Pinto IRCA, Gonzalez ALC, Mendes O Jr (1992) The South Atlantic Magnetic Anomaly: three decades of research. *J Atmos Terr Phys* 54:1129–1134
- Posfai M, Lefevre CT, Trubitsyn D, Bazylinski DA, Frankel RB (2013) Phylogenetic significance of composition and crystal morphology of magnetosome minerals. *Front Microbiol* 4:344
- Silva KT, Abreu F, Almeida FP, Keim CN, Farina M, Lins U (2007) Flagellar apparatus of South-seeking many-celled magnetotactic prokaryotes. *Microsc Res Technol* 70:10–17
- Wiltshcko R, Wiltshcko W (2006) Magnetoreception. *BioEssays* 28:157–168
- Yan L, Zhang S, Chen P, Liu H, Yin H, Li H (2012) Magnetotactic bacteria, magnetosomes and their application. *Microbiol Res* 167:507–519
- Yang C, Chen C, Ma Q, Wu L, Song T (2012) Dynamic model and motion mechanism of magnetotactic bacteria with two lateral flagellar bundles. *J Bionic Eng* 9:200–210
- Zhang WY, Zhou K, Pan HM, Yue HD, Jiang M, Xiao T, Wu LF (2012) Two genera of magnetococci with bean-like morphology from intertidal sediments of the Yellow Sea, China. *Appl Environ Microbiol* 78:5606–5611
- Zhang SD, Petersen N, Zhang WJ, Cargou S, Ruan J, Murat D, Santini CL, Song T, Kato T, Notareschi P, Li Y, Namba K, Gue AM, Wu LF (2014) Swimming behaviour and magnetotaxis function of the marine bacterium strain MO-I. *Environ Microbiol Rep* 6:14–20